Robotica (2008) volume 26, pp. 643–653. © 2008 Cambridge University Press
doi:10.1017/S0263574708004268 Printed in the United Kingdom

Ankle and hip strategies for balance recovery of a biped subjected to an impact

Dragomir N. Nenchev* and Akinori Nishio

Department of Mechanical Systems Engineering, Musashi Institute of Technology, Tokyo 158-8557, Japan

(Received in Final Form: February 6, 2008. First published online: June 4, 2008)

SUMMARY

A humanoid robot should be able to keep balance even in the presence of disturbing forces. Studies of human body reaction patterns to sudden external forces (impacts) are useful for developing balance control strategies. In this paper, we show how to implement two such reaction patterns, called ankle and hip strategy, using a small humanoid robot. Simple dynamical models in the sagittal plane are employed. The decision for invoking one of the reaction patterns is based on acceleration data measured during the impact. The experiments confirm that the robot is able to react swiftly, similar to a human.

KEYWORDS: biped robot; external disturbance; balance recovery; reaction null-space method.

1. Introduction

Humanoid robots are expected to operate within environments shared with humans. Consequently, special attention should be paid to safety of operation—a major problem still to be addressed thoroughly. Under safety of operation we understand not only the problem of how to prevent damage of the robot itself, when it falls down for example,[1] but also first of all, how to prevent the robot from falling down.

Closely related to safety of operation is the problem of balance control. The problem has been fairly well addressed in the case of a regular walking cycle, e.g., based on various Zero Moment Point walking pattern generators.[2,3] In ref. [4] it was shown that when walking on uneven terrain, balance control can be improved by grasping suitable static objects from the environment. Balance control while lifting an object has been addressed in ref. [5]. A few studies tackled the balance problem in light of response to unexpected changes in the environment. Examples include keeping upright posture on changing slopes,[6] walk on uneven terrain,[7] and recently, maintaining balance when an obstacle appears suddenly on the path and the robot has to stop.[8–10]

Another representative example of a balance control problem is quick balance recovery after the robot has been subjected to an unexpected external impact force while standing upright. Such a force could be caused by accidental collisions with humans or other surrounding objects. P. Gorce has addressed the problem via a hierarchical control structure[11] that includes a "coordinator" level with optimization capability based on the Simplex method. It should be noted that human body reaction for recovering balance under similar circumstances has been investigated extensively in the biomechanics and physical therapy literature. As a result, two distinctive patterns of response to the impact, called "ankle" and "hip" strategy, have been recognized.[12–15] Based on these strategies, a continuum of different postural movements can be synthesized.[13] The essential point here is that the center of mass (CoM) stays always within the base of support (BoS). The ankle strategy, for example, displaces the CoM slightly when the standing upright posture is perturbed. It was found out that this strategy is realized through ankle torque only. The hip strategy, on the other hand, minimizes the displacement of the CoM from the vertical by applying a torque in the hips mainly. Note that the response motion pattern depends on the external force applied. With a gentle push on the back, the human body reacts with the ankle strategy. With a stronger push, balance can be maintained by bending in the hips, i.e., with the hip strategy. When the acting force becomes even stronger, then to maintain balance, the BoS has to be changed, e.g., by making a step.

So far, the two strategies have been adapted to bipeds, though only in simulation studies.[16–18] The main emphasis has been put on the hip strategy thereby. Azevedo, Poignet and Espiau[17] derived a postural control method for a seven-joint planar biped using quadratic programming. Abdallah and Goswami[18] proposed a two-phase strategy for balance recovery and applied it to a planar four-link biped. In these works, no attention has been paid to a natural looking balance recovery pattern, as observed in humans, though. In the latter work, for example, one can observe folding of the knee joint in the opposite direction, which leads to an unnatural posture. Another important problem that was not addressed in these works is the problem of transition between postures.

The aim of the present work is to propose a way of implementing the ankle and hip strategies for balance recovery of a biped.[19] As in most of the work done so far, we will rely upon planar dynamical models. Special emphasis will be put on the hip strategy that has drawn the most attention in literature. We will show that a method, developed originally for base disturbance control of free-flying[20] or flexible-base mounted space robots,[21] can be applied in a straightforward manner for balance recovery of a biped under the hip strategy. Further on, the problem of transition between the two balance recovery strategies will be addressed as well. The biped used to confirm expermentally

* Corresponding author. E-mail: nenchev@sc.musashi-tech.ac.jp

the validity of the models is a small humanoid robot HOAP-2 (Fujitsu Automation).[22] The robot's response is in real-time, using a sensor-based approach that allows to initialize the most appropriate balance recovery strategy based on impact force data, obtained from the embedded acceleration sensor of the robot.

The paper is organized as follows. In the following section, the Reaction Null-Space method is overviewed. Section III presents the equation of motion of a biped in a compact form. Thereafter, in Section IV, we introduce the Reaction Null-Space formulation of a biped. Section V discusses the implementation of the ankle and hip strategies. Section VI presents experimental results. Finally, our conclusions are presented in Section VII.

2. Background: Space Robotics and the Reaction Null-Space Method

There are two types of space robots that show similarity to bipeds in the necessity of controls utilizing the force of reaction. The first type includes free-flying space robots, studied extensively during the past two decades with the aim of developing autonomous on-orbit servicing technologies. The lack of a fixed base necessitated research on path planning and control methods for minimizing the base disturbance, induced by reactions due to manipulator motion.[23] The second type of a space robot experiencing a similar problem is the so-called "macro-mini manipulator" system, comprising one or two small manipulators (the "mini" part) mounted on top of a larger manipulator (the "macro" part). The mini manipulator performs dexterous tasks while the macro manipulator ensures a sufficiently large workspace. The latter can be regarded in fact as a flexible support structure for the former. Hence, reactions from mini-manipulator motions may induce vibrations in the flexible macro-manipulator base.[24]

A variety of control algorithms have been developed so far to deal with the base disturbance problem. We draw the reader's attention to model-based control methods that rely upon a proper dynamic model to account for the inertia coupling between the base and the manipulator. One such method is the "Reaction Null-Space" method[†20] shown to be helpful in generating reactionless (mini-)manipulator trajectories for both free-flying space robots and macro-mini space manipulator systems. For the latter systems, the method was also successfully applied to damp out existing vibrations in the flexible support base, controlling the mini-manipulator induced reactions in an optimal way.[21]

The equation of motions of both types of space robots have the same structure:

$$\begin{bmatrix} \boldsymbol{H}_b & \boldsymbol{H}_{bm} \\ \boldsymbol{H}_{bm}^T & \boldsymbol{H}_m \end{bmatrix} \begin{bmatrix} \dot{\boldsymbol{v}}_b \\ \ddot{\boldsymbol{\theta}} \end{bmatrix} + \begin{bmatrix} \boldsymbol{c}_b \\ \boldsymbol{c}_m \end{bmatrix} = \begin{bmatrix} \boldsymbol{0} \\ \boldsymbol{\tau} \end{bmatrix} + \begin{bmatrix} \boldsymbol{J}_{bm}^T \\ \boldsymbol{J}^T \end{bmatrix} \boldsymbol{w}, \qquad (1)$$

where

$\boldsymbol{\theta}$	$\in \Re^n$	Joint angle vector
$\boldsymbol{v}_b$	$\in \Re^6$	Base spatial velocity (twist)
$\boldsymbol{H}_m$	$\in \Re^{n\times n}$	Manipulator inertia matrix
$\boldsymbol{H}_b$	$\in \Re^{6\times 6}$	Base inertia matrix
$\boldsymbol{H}_{bm}$	$\in \Re^{6\times n}$	Inertia coupling matrix
$\boldsymbol{c}_m$	$\in \Re^n$	Velocity dependent nonlinear joint torque
$\boldsymbol{c}_b$	$\in \Re^6$	Velocity dependent nonlinear force/ moment (wrench) at the base
$\boldsymbol{J}$	$\in \Re^{6\times n}$	Manipulator Jacobian matrix
$\boldsymbol{J}_{bm}$	$\in \Re^{6\times 6}$	Force transform
$\boldsymbol{\tau}$	$\in \Re^n$	Manipulator joint torque
$\boldsymbol{w}$	$\in \Re^6$	End-link force/moment (wrench).

The upper part of the equation of motion relates all forces acting at the base:

$$\boldsymbol{H}_b \dot{\boldsymbol{v}}_b + \boldsymbol{H}_{bm} \ddot{\boldsymbol{\theta}} + \boldsymbol{c}_b - \boldsymbol{J}_{bm}^T \boldsymbol{w} = \boldsymbol{0}. \qquad (2)$$

Let us assume a stationary initial state and no external forces at the end-link ($\boldsymbol{w} = \boldsymbol{0}$). Then, the condition for maintaining the stationary state of the base is obtained from the last equation, as:

$$\boldsymbol{H}_{bm} \ddot{\boldsymbol{\theta}} + \dot{\boldsymbol{H}}_{bm} \dot{\boldsymbol{\theta}} = \boldsymbol{0}. \qquad (3)$$

Note that the velocity-dependent nonlinear force/moment vector $\boldsymbol{c}_b$ has been approximated as $\dot{\boldsymbol{H}}_{bm}\dot{\boldsymbol{\theta}}$. Next, integrate the last equation, to obtain:

$$\boldsymbol{H}_{bm} \dot{\boldsymbol{\theta}} = \boldsymbol{L}. \qquad (4)$$

The integration constant $\boldsymbol{L}$ has the meaning of momentum and has been named the *coupling momentum*.[20] It becomes apparent that to maintain the state of the base, the coupling momentum should be conserved.

Joint accelerations and joint velocities that do not disturb the base are obtained from Eqs. (3) and (4), respectively. These equations are underdetermined, under the condition $n > 6$. Hence, infinite sets of solutions exist:

$$\ddot{\boldsymbol{\theta}} = -\boldsymbol{H}_{bm}^{+} \dot{\boldsymbol{H}}_{bm} \dot{\boldsymbol{\theta}} + (\boldsymbol{I} - \boldsymbol{H}_{bm}^{+} \boldsymbol{H}_{bm}) \boldsymbol{\xi}_2 \qquad (5)$$

and

$$\dot{\boldsymbol{\theta}} = (\boldsymbol{I} - \boldsymbol{H}_{bm}^{+} \boldsymbol{H}_{bm}) \boldsymbol{\xi}_1, \qquad (6)$$

respectively. Here, $\boldsymbol{H}_{bm}^{+} \in \Re^{n\times 6}$ denotes the pseudoinverse matrix, $\boldsymbol{\xi}_1, \boldsymbol{\xi}_2 \in \Re^n$ are arbitrary vectors, $(\boldsymbol{I} - \boldsymbol{H}_{bm}^{+} \boldsymbol{H}_{bm})$ is a null space projector. The integration constant $\boldsymbol{L}$ was assumed zero (a stationary initial state). The null space of the inertia coupling matrix $\boldsymbol{H}_{bm}$ has been named the *Reaction Null-Space*.[20] Manipulator joint accelerations/velocities from within this space guarantee zero reaction at the base.

There are two particular cases of special interest.

Case 1. Sometimes, just a partial state constraint is to be imposed instead of the full constraint, as in Eq. (3) (or Eq. (4)). For example, in case of the free-flying space robot discussed here, the rotation of the base plays a much more important role than its translation. Then, we would like to formulate a Reaction Null-Space in terms of base rotations.

[†] Introduced initially as the FAR-Jacobian method in.[25]

This can be done in a straightforward manner by collecting only those components from the equation of base motion (2), that are related to rotational motion, and by then applying the same procedure as above. We refer to this method as the *selective* Reaction Null-Space (see[21] for further details).

Case 2. Note the possibility to change the state of the base via manipulator motion, in the absence of external forces. This can be done with the following joint acceleration:

$$\ddot{\boldsymbol{\theta}} = -\boldsymbol{H}_{bm}^{+}(\boldsymbol{H}_b\dot{\boldsymbol{v}}_b + \boldsymbol{c}_b) + (\boldsymbol{I} - \boldsymbol{H}_{bm}^{+}\boldsymbol{H}_{bm})\boldsymbol{\xi}_2, \qquad (7)$$

where $\dot{\boldsymbol{v}}_b$ denotes the base spatial acceleration that would ensure the desired state of the base. Note that, with $\boldsymbol{\xi}_2 = \boldsymbol{0}$, the above solution is locally optimal.[‡] This method has been used to exchange partial (base and manipulator) angular momenta within the free-flying space robot, after an impact has occured at the manipulator hand.[20]

Now, let us return to the statement in the beginning of this section, about the similarity between space robots, of the types discussed, and bipeds. When no external disturbances are present, a biped can maintain balance, provided the total wrench on the supporting foot/feet is zero. This can be ensured both in the trivial case of a stationary state (static balance), and also in the nontrivial case of dynamic balance. By making the parallel between the base of the space robot and the foot/feet of the biped on one side, and between the manipulator(s) of the space robot and the rest of the links of the biped, on the other side, it should be apparent that the Reaction Null-Space notation would provide the necessary condition for maintaining the balance of the biped. In other words, joint accelerations and joint velocities, that do not disturb the state of the support foot/feet of the biped, can be obtained in the form of Eqs. (5) and (6), respectively. Also, one can predict the existence of a "coupling momentum" of a biped, similar to the coupling momentum in Eq. (4). Moreover, note that usually, sufficiently large friction forces are assumed at the feet, so that we can ignore three of the wrench components: the moment around the vertical and the two forces in the orthogonal directions. This means that the concept of the selective Reaction Null-Space would be applicable. Further details are given in the next two sections.

3. Equation of Motion of a Biped

A biped maintains balance through proper control of the reaction wrench at the support foot. The reaction is clearly related to the wrench imposed on the foot by the movements of all links, by gravity, and by other external forces acting on the biped. Hence, control of the imposed wrench is of primary importance.

To ensure such control, we envision the adaptation of the Reaction Null-Space method introduced in the previous section. The support foot/feet play the role of a "base," while the rest of the links of the biped play the role of the "manipulator" in the equation of motion (1).

[‡] This follows directly from the well-known fact that the pseudoinverse-based particular solution has a minimum norm.

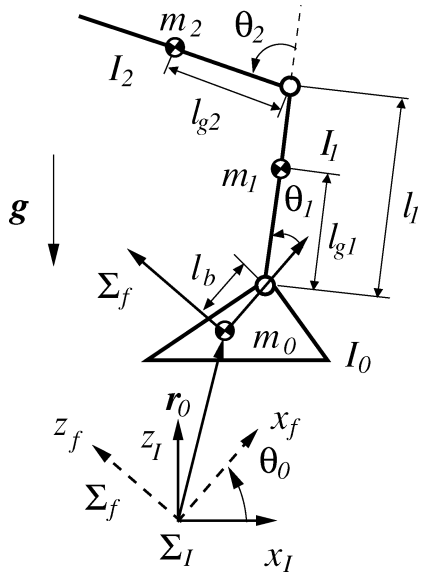

Fig. 1. Model of a planar biped in midair.

As an illustrative example, we consider a simple three-link planar model in the sagittal plane, comprising the foot, the lower body (leg), and the upper body (see Fig. 1). The joint at the foot is the ankle joint (angle θ_1), the other joint is the "hip joint."

The equation of motion of the three link model can be written as follows:

$$\begin{bmatrix} \boldsymbol{H}_f & \boldsymbol{H}_{fl} \\ \boldsymbol{H}_{fl}^T & \boldsymbol{H}_l \end{bmatrix} \begin{bmatrix} \dot{\boldsymbol{v}} \\ \ddot{\boldsymbol{\theta}} \end{bmatrix} + \begin{bmatrix} \boldsymbol{c}_f \\ \boldsymbol{c}_l \end{bmatrix} + \begin{bmatrix} \boldsymbol{g}_f \\ \boldsymbol{g}_l \end{bmatrix} = \begin{bmatrix} \boldsymbol{0} \\ \boldsymbol{\tau} \end{bmatrix} + \begin{bmatrix} \boldsymbol{J}_{fp}^T \\ \boldsymbol{J}^T \end{bmatrix} \begin{bmatrix} \boldsymbol{f} \\ n \end{bmatrix} \qquad (8)$$

where

$\boldsymbol{\theta}$	$\in \Re^2$	Joint angle vector
$\boldsymbol{v}$	$\in \Re^3$	Foot velocity (angular speed incl.)
$\boldsymbol{H}_l$	$\in \Re^{2\times 2}$	Leg and upper body inertia matrix
$\boldsymbol{H}_f$	$\in \Re^{3\times 3}$	Foot inertia matrix
$\boldsymbol{H}_{fl}$	$\in \Re^{3\times 2}$	Inertia coupling matrix
$\boldsymbol{c}_l$	$\in \Re^2$	Velocity dependent nonlinear joint torque
$\boldsymbol{c}_f$	$\in \Re^3$	Velocity dependent nonlinear wrench at the foot
$\boldsymbol{g}_l$	$\in \Re^2$	Gravity joint torque
$\boldsymbol{g}_f$	$\in \Re^3$	Gravity wrench at the foot
$\boldsymbol{\tau}$	$\in \Re^2$	Joint torque vector.

Assume that an external wrench $[\boldsymbol{f}^T \;\; n]^T$ is applied at the upper body link at a point displaced by a units from the CoM of this link outward. Figure 2 illustrates the static forces on the model. The *imposed wrench* at the foot $[\boldsymbol{f}_f^T \;\; n_f]^T$ and the static joint torque $\boldsymbol{\tau}' = [\tau_1' \;\; \tau_2']^T$, appearing in the right-hand-side of Eq. (8), are:

$$\begin{bmatrix} \boldsymbol{f}_f \\ n_f \\ \boldsymbol{\tau}' \end{bmatrix} = \begin{bmatrix} \boldsymbol{J}_{fp}^T \\ \boldsymbol{J}^T \end{bmatrix} \begin{bmatrix} \boldsymbol{f} \\ n \end{bmatrix}, \qquad (9)$$

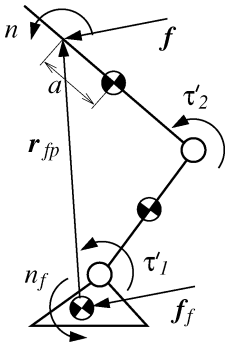

Fig. 2. Static force model.

where

$$\boldsymbol{J}_{fp}^{T} = \begin{bmatrix} \boldsymbol{I}_{2\times 2} & \boldsymbol{0} \\ [\boldsymbol{r}_{fp}\times] & 1 \end{bmatrix} = \begin{bmatrix} 1 & 0 & 0 \\ 0 & 1 & 0 \\ -r_{fpz} & r_{fpx} & 1 \end{bmatrix}, \tag{10}$$

$$\boldsymbol{r}_{fp} = \begin{bmatrix} x_b + l_1 C_1 + (l_{g2} + a) C_{12} \\ l_1 S_1 + (l_{g2} + a) S_{12} \end{bmatrix} \tag{11}$$

and the Jacobian matrix for the point where the wrench is applied, is:

$$\boldsymbol{J} = \begin{bmatrix} -l_1 S_1 - (l_{g2} + a) S_{12} & -(l_{g2} + a) S_{12} \\ l_1 C_1 + (l_{g2} + a) C_{12} & (l_{g2} + a) C_{12} \\ 1 & 1 \end{bmatrix}. \tag{12}$$

In the above equations, $S_1 = \sin\theta_1$, $C_1 = \cos\theta_1$, $S_{12} = \sin(\theta_1 + \theta_2)$, $C_{12} = \cos(\theta_1 + \theta_2)$.

4. The Reaction Null-Space of Bipeds

Assume a biped in balance with motionless support foot and vertical reaction passing through the CoM. Such a state can be easily maintained, provided the imposed wrenches at the support foot, resulting from link motions, are summed up to zero. Following the Reaction Null-Space method described in Subsection 2, it is straightforward to obtain all joint accelerations/velocities that would maintain the balance, as:

$$\ddot{\boldsymbol{\theta}} = -\boldsymbol{H}_{fl}^{+} \dot{\boldsymbol{H}}_{fl} \dot{\boldsymbol{\theta}} + (\boldsymbol{I} - \boldsymbol{H}_{fl}^{+} \boldsymbol{H}_{fl}) \boldsymbol{\xi}_2 \tag{13}$$

and

$$\dot{\boldsymbol{\theta}} = (\boldsymbol{I} - \boldsymbol{H}_{fl}^{+} \boldsymbol{H}_{fl}) \boldsymbol{\xi}_1, \tag{14}$$

respectively. Note also that the joint velocity in the last equation conserves the coupling momentum at zero: $\boldsymbol{H}_{fl} \dot{\boldsymbol{\theta}} = \boldsymbol{0}$.

A necessary condition for the existence of the Reaction Null-Space is that the number of joints n is larger than the DOF's of the foot. Note that this is *not* the case with the planar model introduced in the previous section. Indeed, the inertia coupling matrix $\boldsymbol{H}_{fl}$ is 3×2, and we have an underactuated system at hand. We can make use of the selective Reaction Null-Space, though, to control particular component(s) of the reaction.

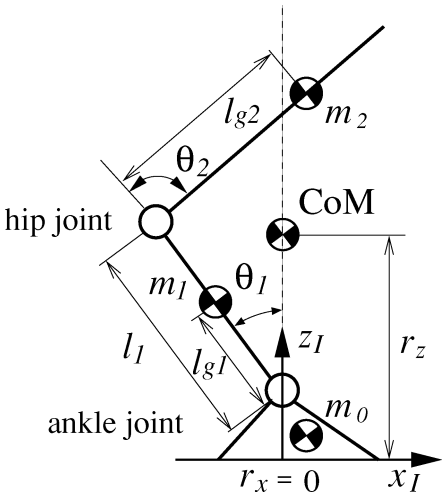

Fig. 3. Three-link model of grounded planar biped.

Consider the model shown in Fig. 3. This is the same three-link model as already described, but now attached to the ground. With this model, balance will be ensured by always keeping the total CoM on the vertical. In other words, we will ignore the imposed force component in the z direction and the moment component n_f (cf. Fig. 2). Hence, the selective Reaction Null-Space will be applied to control the imposed force component in the x direction only.

Denote by $\boldsymbol{r}$ the position of the CoM, with components:

$$\begin{aligned} r_x &= \frac{m_1 l_{g1} S_1 + m_2 (l_1 S_1 + l_{g2} S_{12})}{m_1 + m_2} \\ r_z &= \frac{m_1 l_{g1} C_1 + m_2 (l_1 C_1 + l_{g2} C_{12})}{m_1 + m_2}. \end{aligned} \tag{15}$$

The initial condition $r_x = 0$ will be maintained to ensure that the speed $\dot{r}_x$ is zero throughout the motion. The velocity of

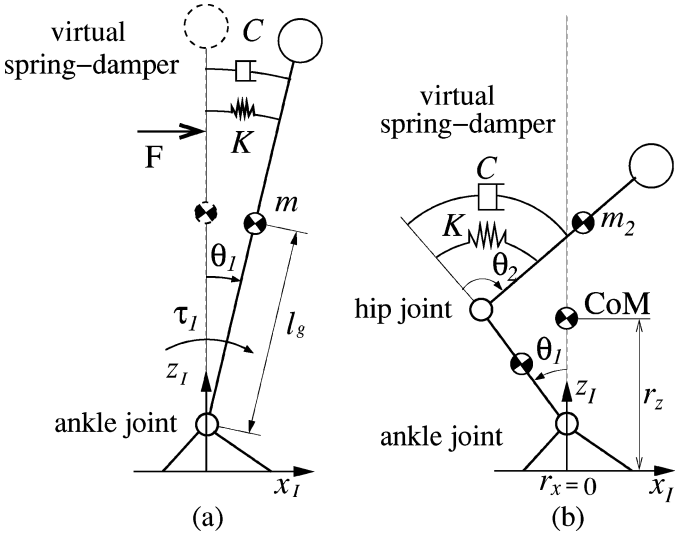

Fig. 4. Models for the (a) ankle and (b) hip strategies.

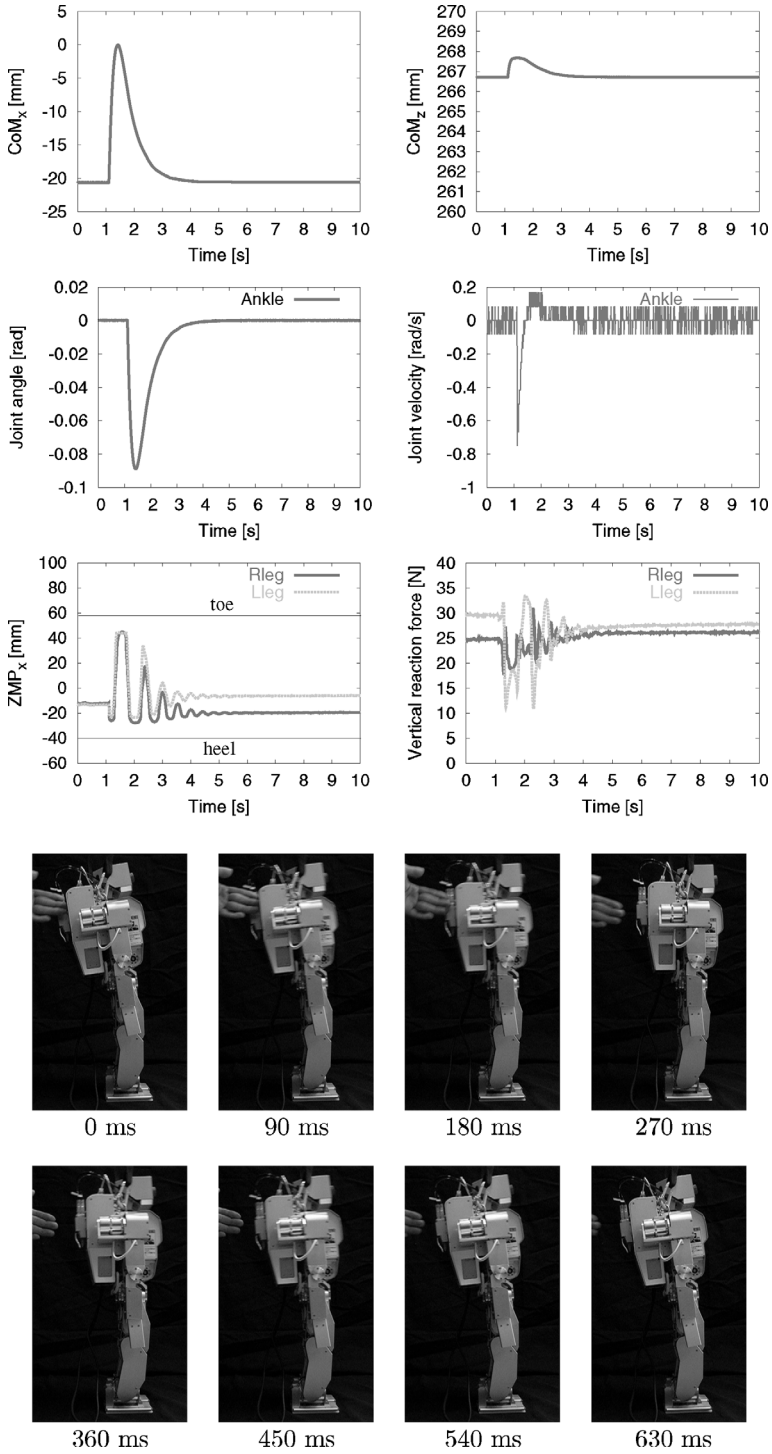

Fig. 5. Ankle strategy with success.

the CoM is:

$$\begin{bmatrix} \dot{r}_x \\ \dot{r}_z \end{bmatrix} = \begin{bmatrix} r_z & \dfrac{m_2 l_{g2} C_{12}}{m_1 + m_2} \\ -r_x & -\dfrac{m_2 l_{g2} S_{12}}{m_1 + m_2} \end{bmatrix} \begin{bmatrix} \dot{\theta}_1 \\ \dot{\theta}_2 \end{bmatrix}. \tag{16}$$

The CoM motion constraint is obtained from the x component of the above equation, as:

$$\begin{bmatrix} r_z & \dfrac{m_2 l_{g2} C_{12}}{m_1 + m_2} \end{bmatrix} [\dot{\theta}_1 \quad \dot{\theta}_2]^T = 0. \tag{17}$$

From the row-matrix in the last equation, we obtain the inertia coupling matrix in terms of the selective Reaction Null-Space, as $\boldsymbol{H}_{fl} = [r_z(m_1 + m_2) \quad m_2 l_{g2} C_{12}]$. There is one nonzero vector in the kernel of this matrix. Hence, the selective Reaction Null-Space contains the set of joint velocities:

$$\dot{\boldsymbol{\theta}} = b\boldsymbol{n}, \tag{18}$$

where b is an arbitrary scalar, and the null-space vector is

$$\boldsymbol{n} = \begin{bmatrix} -m_2 l_{g2} C_{12} \\ (m_1 l_{g1} + m_2 l_1) C_1 + m_2 l g_2 C_{12} \end{bmatrix}. \tag{19}$$

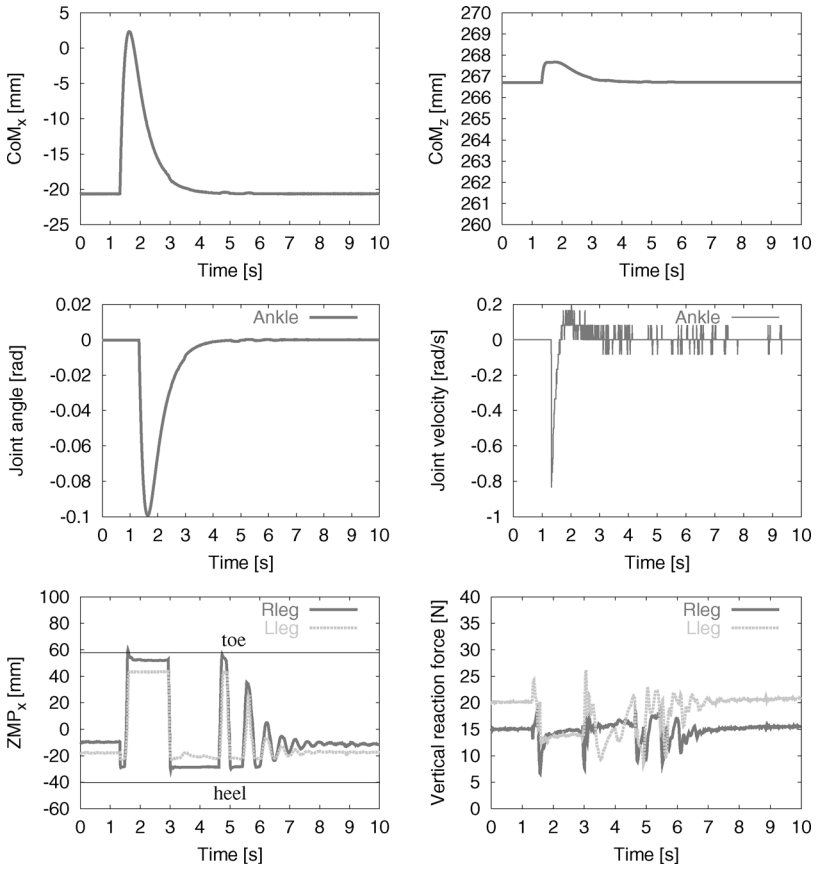

Fig. 6. Ankle strategy without success.

Finally, eliminate b from the last two equations to obtain the following relation between the two joint speeds:

$$\dot{\theta}_1 = \frac{-m_2 l_{g2} C_{12}}{(m_1 l_{g1} + m_2 l_1) C_1 + m_2 l_{g2} C_{12}} \dot{\theta}_2. \tag{20}$$

5. Sensor-Based Response Strategies for HOAP-2

We implemented the ankle and hip strategies to control postural balance of a small humanoid robot HOAP-2,[22] subjected to an impact force while standing upright. As already explained, the strategies differ in how they control joint and CoM motions: the ankle strategy displaces the CoM (within the BoS) by ankle joint movement, while the hip strategy minimizes CoM displacement from the vertical by movements in both ankle and hip joints. Thus, we will need two different models to realize the strategies. It will be shown, thereby, that it is possible to rely on just simple planar dynamical models.

Figure 4 shows the models for the ankle and hip strategies. Both models include a spring-damper to ensure compliance with the impact force, either by ankle motion (Fig. 4(a)), or by hip/ankle motion (Fig. 4(b)).

The impact force is evaluated via the acceleration sensor, embedded in the chest of HOAP-2. The data is then used to decide which one of the **two** strategies is to be invoked. For this purpose, we determined experimentally a threshold for the impact acceleration. Impacts, with acceleration values below/above the threshold, invoke the ankle/hip strategy, respectively.

5.1. Ankle strategy implementation

It should be apparent that the ankle strategy is modeled after an inverted pendulum. The equation of motion is:

$$I\ddot{\theta}_1 - mgl_g \sin\theta_1 = -C\dot{\theta}_1 - K\theta_1, \tag{21}$$

where $I \equiv I' + ml_g^2$, I' is the moment of inertia, and the other parameters are obvious form the model (see Fig. 4 (a)). This equation is simplified by ignoring the gravity term, which is justified by the high gear ratios and the internal high-gain feedback controller of HOAP-2. Hence, we obtain the reference ankle joint acceleration from the above equation as:

$$\ddot{\theta}_1^{\text{ref}} = -(C\dot{\theta}_1 + K\theta_1)/I. \tag{22}$$

Further on, the moment balance equation during impact can be written as

$$I\ddot{\theta}_1 = mal_g, \tag{23}$$

where a is the measured acceleration. Assuming a small impact time interval Δt, and using the relation $\ddot{\theta}_1 = \Delta\dot{\theta}_1/\Delta t$, we obtain the ankle joint angular speed step change as

$$\Delta\dot{\theta}_1 = mal_g \Delta t/I. \tag{24}$$

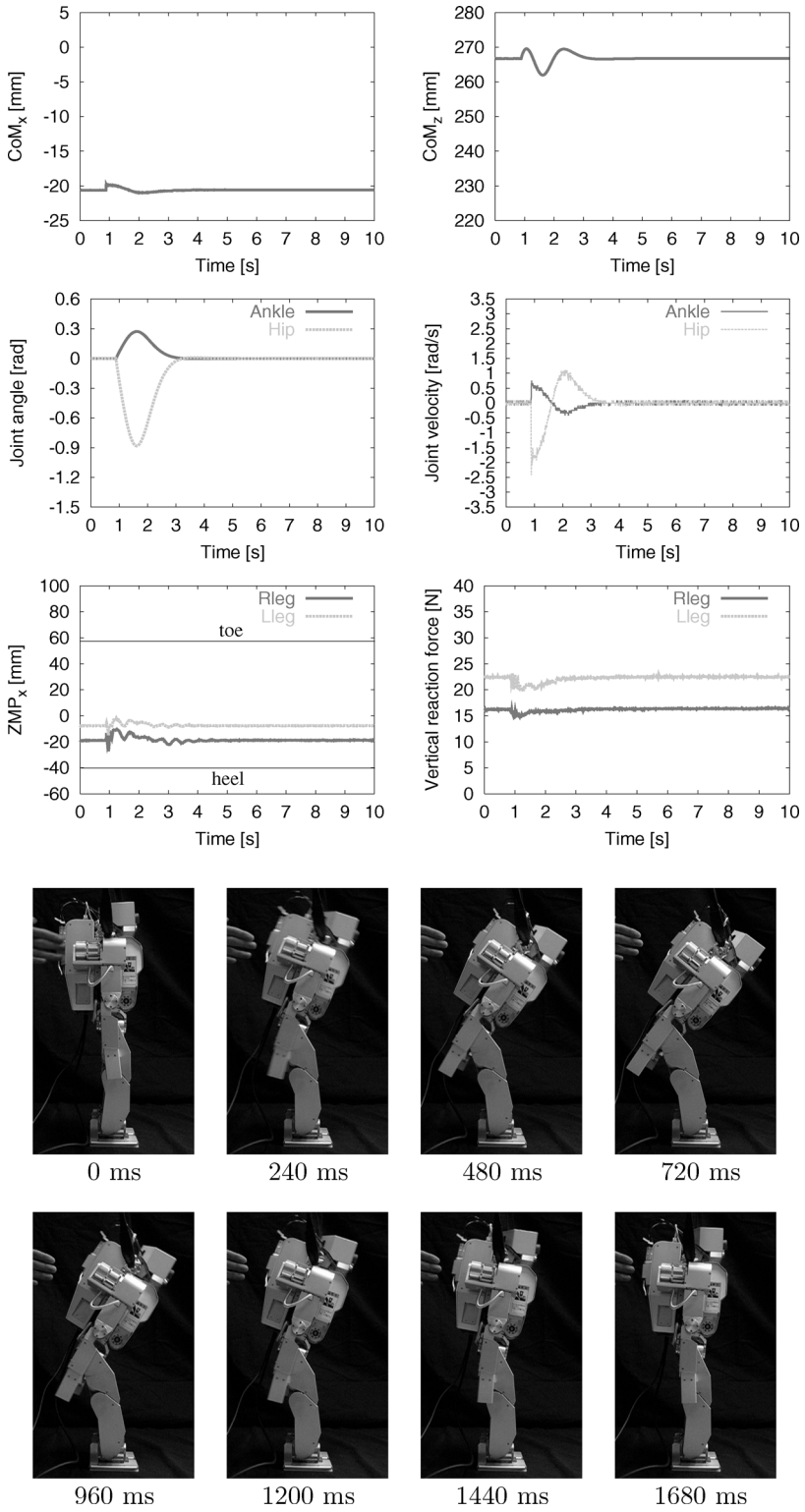

Fig. 7. Hip strategy under a relatively weak force on the back.

The step change determines the initial state for the post-impact motion. The latter is calculated from the joint acceleration in (22). The acceleration is then integrated twice to obtain the reference ankle joint angle $\theta_1^{\text{ref}}(t)$, which is then fed to HOAP-2's internal controller for execution. With this method, the robot reacts faster to larger impact forces.

5.2. Hip strategy implementation

The reference trajectories for the hip joint $\ddot{\theta}_2^{\text{ref}}(t)$, $\dot{\theta}_2^{\text{ref}}(t)$, $\theta_2^{\text{ref}}(t)$ are calculated in the same way as in the ankle strategy, based on an initial state obtained from the acceleration sensor, and on post-impact hip-joint acceleration determined from the spring-damper equation.

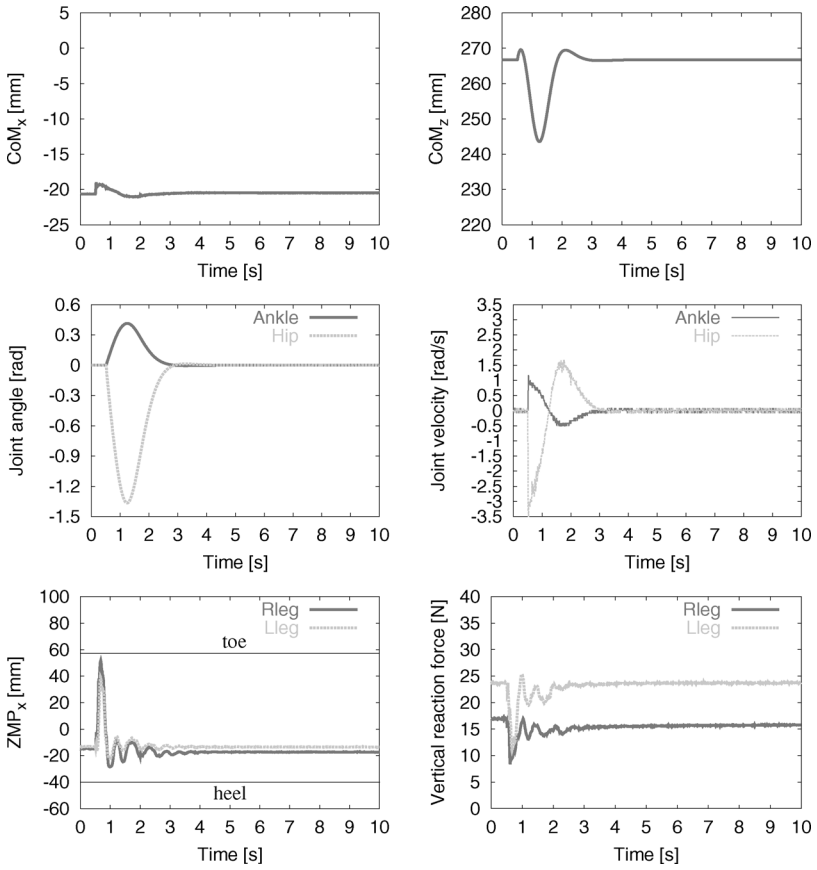

Fig. 8. Hip strategy under a relatively strong force on the back.

Once the reference trajectories for the hip joint are known, it is straightforward to apply the selective Reaction Null-Space method, by determining the proper motion in the ankle joint $\dot{\theta}_1^{\text{ref}}(t)$, from Eq. (20).

6. Experiments

A set of experiments for the two strategies have been performed with a small-size humanoid robot (HOAP-2).

6.1. Ankle strategy experiment

The dynamic parameters for the inverted pendulum model are calculated based on HOAP-2's data, as $I' = 0.101\,\text{kgm}^2$, $l_g = 0.239\,\text{m}$, and $m = 6.75\,\text{kg}$. The robot was subjected to an impact force by hand on the back. The impact time interval was selected as $\Delta t = 1\,\text{ms}$.

In order to obtain a satisfactory behavior, we had to use time-variable spring-damper coefficients $C(t)$ and $K(t)$, derived from 5th order polynomials. The initial and final values of the coefficients were determined experimentally as $K^{init} = 5.0\,\text{Nm/rad}$, $K^{final} = 8.0\,\text{Nm/rad}$, and $C^{init} = 3.0\,\text{Nms/rad}$, $C^{final} = 5.0\,\text{Nms/rad}$, respectively. The final time t_f for the polynomials was selected as $t_f = 1.0\,\text{s}$.

The experimental data graphs and corresponding snapshots of HOAP-2's motion for an impact acceleration of $a = 0.89\,\text{m/s}^2$, are shown in Fig. 5. It is seen that the displacement of the CoM is predominantly in the x direction. The step change in angular speed is about $-0.75\,\text{rad/s}$. The ZMP graph shows that the ZMP remains within the BoS (between the "heel" and "toe" lines in the graph), and that the balance recovery pattern is stable. The data in the ZMP graph, as well as these in the vertical reaction force graph, are calculated from the pressure sensors of the left and the right foot. Note that the robot is not perfectly symmetrical, therefore, one should not expect perfect match for left and right, even in the case of a planar model.

We made another experiment to demonstrate how the reaction pattern changes with a larger impact force. Figure 6 shows the data graphs for an impact acceleration of $a = 1.00\,\text{m/s}^2$. Though the step change in angular speed seems to be just a bit larger than in the previous experiment, from the ZMP graph it is apparent that the ZMP stays for relatively longer time, first at the "toe" boundary, than at the "heel" boundary. This indicates posture instability and we can conclude that the robot was not able to maintain balance under the ankle strategy. We can also conclude that the impact acceleration threshold for invoking the hip strategy should be less than the critical impact acceleration used in this experiment.

6.2. Hip strategy experiment

The kinematic and dynamic parameters for the hip strategy model (cf. Fig. 4(b)) are shown in Table I. Here also,

Table I. Link parameters for the hip strategy model.

Parameter Unit	m [kg]	I [kgm^2]	l [mm]	l_g [mm]
Link 1	1.450	0.0057789	200	82.05
Link 2	4.961	0.03214829		10.251

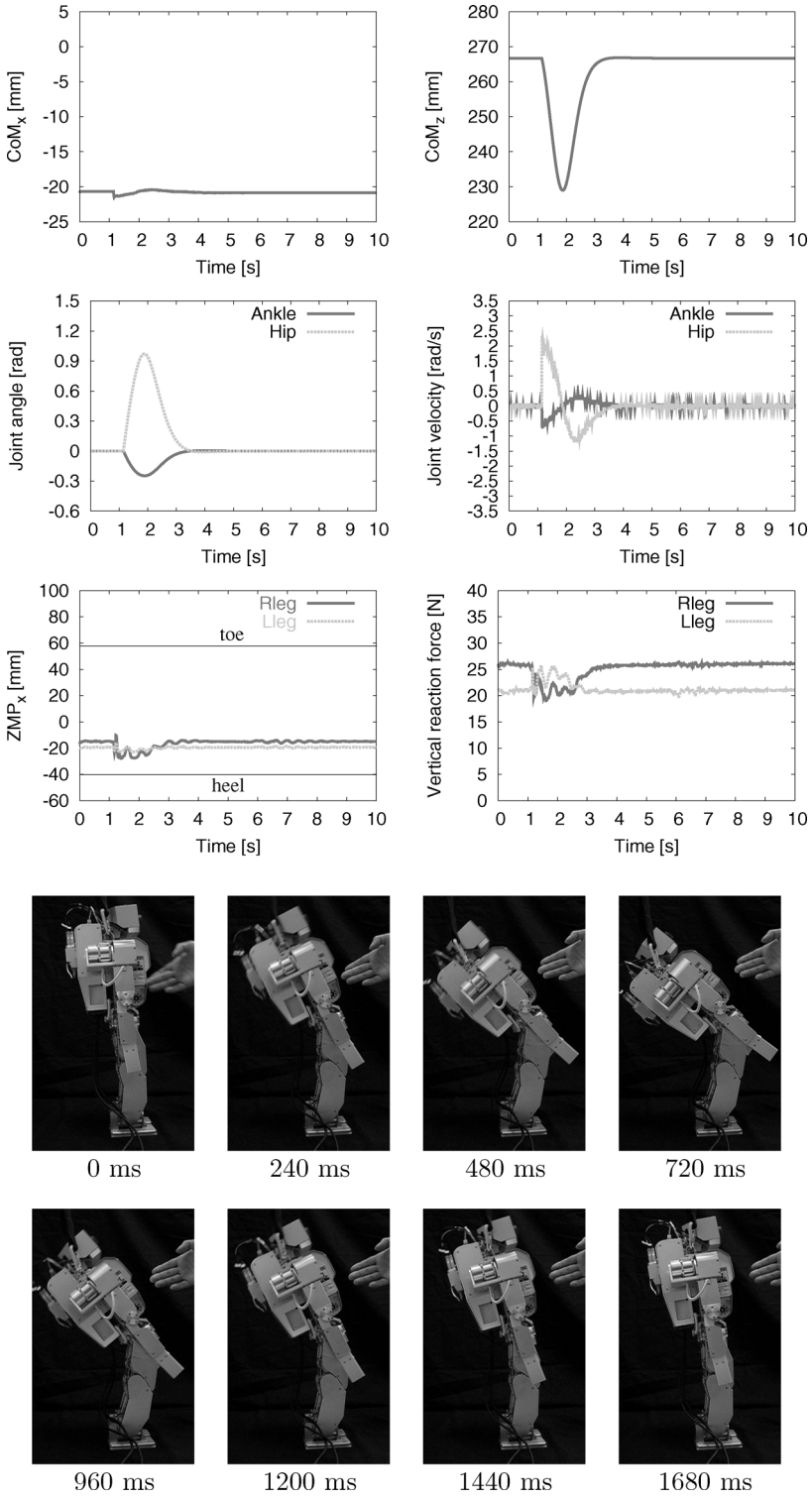

Fig. 9. Hip strategy under an impact on the chest.

time-variable spring-damper coefficients had to be used. The initial and final values for the 5th order polynomials for the coefficients were determined experimentally as $K^{init} = 0.1\,\text{Nm/rad}$, $K^{final} = 0.7\,\text{Nm/rad}$, and $C^{init} = 0.06\,\text{Nms/rad}$, $C^{final} = 0.4\,\text{Nms/rad}$, respectively. The final time t_f for the polynomials was selected as $t_f = 1.5\,\text{s}$.

We performed three experiments. In the first experiment, the impact force was applied from the back, yielding an impact acceleration of $a = 0.97\,\text{m/s}^2$. This is slightly below the acceleration of $a = 1.00\,\text{m/s}^2$ for which the robot could not maintain balance during the second ankle strategy experiment (the case without success). As can be seen from the experimental data graphs and the corresponding snapshots in Fig. 7, the robot is able to keep balance under the hip strategy. The CoM is thereby only slightly displaced from the vertical. The variation of the ZMP is also quite small. From this experiment, we can conclude that the acceleration

threshold for invoking the hip strategy should be set to less than 0.97 m/s^2.

In the next experiment, a stronger impact force was applied from the back, imposing an impact acceleration of $a = 2.48$ m/s^2. The respective graphs are shown in Fig. 8. It is apparent that the CoM is displaced mainly in the vertical z direction. The motion in the hip joint is quite quick, as seen from the joint velocity graph. The ZMP graph shows that despite the swift reaction, the robot is able to maintain balance. The ZMP is displaced significantly and almost reaches the toe tip. Hence, the impact force in this experiment can be considered as the limit for the hip strategy.

In the final experiment under the hip strategy, the impact force was applied to the chest of the robot. The acceleration was $a = -1.07$ m/s^2, which implies a relatively weak force. The respective graphs and snapshots are shown in Fig. 9. It is seen that the robot reacts in bending in the appropriate direction, with insignificant displacement of the ZMP. We can conclude then that the balance in this case can be maintained as well.

7. Conclusions

The paper illustrated how the ankle and hip strategies—two well-known reaction patterns for balance recovery of a human subjected to a sudden external force while standing upright—can be modeled and applied to a biped. Each of the two strategies was modeled by a simple planar dynamical model in the sagittal plane. In the case of the hip strategy, especially, we adopted the Reaction Null-Space method—a method developed originally for free-flying and flexible-base space robots. The method can be applied to control balance in response to other external perturbations as well, and is easily extendable to the general, three-dimensional case.

We have shown that the impact acceleration data, measured during posture perturbation, can be used in two ways: (1) to modify the speed of reaction for the specific reaction pattern, and (2) to invoke one of the two strategies, depending on the experimentally determined threshold. Our models include virtual spring-dampers used to generate reference trajectories for the reaction patterns. Since our goal was to mimic human behavior, and no appropriate data was available, we had to set the respective parameters on an empirical basis. Further analysis is needed, though, to devise a method for this purpose. Also, in a future work, we plan to make use of impact impulse data, in addition to the impact acceleration, and to enlarge the set of reaction patterns.

References

1. K. Fujiwara, F. Kanehiro, S. Kajita, K. Kaneko, K. Yokoi and K. H. Hirukawa, "UKEMI: Falling Motion Control to Minimize Damage to Biped Humanoid Robot," *Proceedings of the 2002 IEEE International Conference on Intelligent Robots and Systems*, EPFL, Lausanne, Switzerland (Oct. 2002) pp. 2521–2526.
2. S. Kajita, F. Kanehiro, K. Kaneko, K. Fujiwara, K. Harada, K. Yokoi and K. H. Hirukawa, "Biped Walking Pattern Generation by using Preview Control of Zero–Moment Point," *Proceedings of the 2003 IEEE International Conference on Robotics and Automation*, Taipei, Taiwan, Sep. 14–19, (2003) pp. 1620–1626.
3. T. Sugihara, Y. Nakamura and H. Inoue, "Realtime Humanoid Motion Generation through ZMP Manipulation based on Inverted Pendulum Control," *Proceedings of the 2002 IEEE International Conference on Robotics and Automation*, Washington DC, USA, (May 2002) pp. 1404–1409.
4. K. Harada, H. Hirukawa, F. Kanehiro, K. Fujiwara, K. Kaneko, S. Kajita and M. Nakamura, "Dynamical Balance of a Humanoid Robot Grasping an Environment," *Proceedings of the 2004 IEEE International Conference on Intelligent Robots and Systems*, Sendai, Japan, (Sept.–Oct., 2004) pp. 1167–1173.
5. K. Harada, S. Kajita, H. Saito, M. Morisawa, F. Kanehiro, K. Fujiwara, K. Kaneko and H. Hirukawa,"A Humanoid Robot Carrying a Heavy Object," *Proceedings of the 2005 IEEE International Conference on Robotics and Automation*, Barcelona, Spain, (April 2005) pp. 1712–1717.
6. J. S. Gutmann, M. Fukuchi and M. Fujita, "Stair Climbing for Humanoid Robots Using Stereo Vision" *Procedings of the 2004 IEEE International Conference on Intelligent Robots and Systems*, Sendai, Japan, (Sept.–Oct., 2004) pp. 1407–1413.
7. S. Kajita, M. Morisawa, K. Harada, K. Kaneko, F. Kanehiro, K. Fujiwara and H. Hirukawa,"Biped Walking Pattern Generator allowing Auxiliary ZMP Control," *Proceedings of the 2006 IEEE International Conference on Intelligent Robots and Systems*, Beijing, China, (Oct. 2006) pp. 2993–2999.
8. M. Morisawa, K. Kaneko, F. Kanehiro, S. Kajita, K. Fujiwara, K. Harada and H. Hirukawa, "Motion Planning of Emergency Stop for Humanoid Robot by State Space Approach," *Proceedings of the 2006 IEEE International Conference on Intelligent Robots and Systems*, Beijing, China, (Oct. 2006) pp. 2986–2992.
9. T. Tanaka, T. Takubo, K. Inoue and T. Arai, "Emergent stop for Humanoid Robots," *Proceedings of the 2006 IEEE International Conference on Intelligent Robots and Systems*, Beijing, China, (Oct. 2006) pp. 3970–3975.
10. K. Kaneko, F. Kanehiro, S. Kajita, M. Morisawa, K. Fujiwara, K. Harada and H. Hirukawa,"Motion Suspension System for Humanoids in case of Emergency – Real-time Motion Generation and Judgment to suspend Humanoid –," *Proceedings of the 2006 IEEE International Conference on Intelligent Robots and Systems*, Beijing, China, (Oct. 2006) pp. 5496–5503.
11. P. Gorce, "Dynamic postural control method for biped in unknown environment," IEEE Trans. SMC, Part A: Syst. Hum. **29**(6), 616–626 (Nov. 1999).
12. L. M. Nashner and G. McCollum, "The organization of human postural movements: A formal basis and experimental hypothesis," Behav. Brain Sci. **8**, 135–172 (1985).
13. F. B. Horak and L. M. Nashner, "Central programming of postural movements: Adaptation to altered support surface configurations," J. Neurophysiol. **55**(6), 1369–1381 (1986).
14. A. Shumway–Cook and F. B. Horak, "Vestibular rehabilitation: An exercise approach to managing symptoms of vestibular dysfunction," Seminars in Hearing, **10**(2), 196–209 (1989).
15. A. D. Kuo, "An optimal control model for analyzing human postural balance," IEEE Trans. Biomed. Eng., **42**(1), 87–101 (1995).
16. M. Guihard and P. Gorce, "Dynamic Control of Bipeds Using Ankle and Hip Strategies," *Proceedings of the 2002 IEEE International Conference on Intelligent Robots and Systems*, EPFL, Lausanne, Switzerland, (Oct. 2002) pp. 2587–2592.
17. C. Azevedo, P. Poignet and B. Espiau, "Artificial locomotion control: From human to robots," Robot. Auton. Syst. **47**(4), 203–223 (2004).
18. M. Abdallah and A. Goswami, "A Biomechanically Motivated Two-Phase Strategy for Biped Upright Balance Control," *Proceedings of the 2005 IEEE International Conference on Robotics and Automation*, Barcelona, Spain, (April 2005) pp. 1996–2001.
19. A. Nishio, K. Takahashi and D. N. Nenchev, "Balance Control of a Humanoid Robot Based on the Reaction Null Space Method," *Proceedings of the 2006 IEEE International Conference on Intelligent Robots and Systems*, Beijing, China, (Oct. 2006) pp. 1996–2001.

20. D. N. Nenchev and K. Yoshida, "Impact analysis and post-impact motion control issues of a free–floating space robot subject to a force impulse," IEEE Trans. Robot. Autom. **15**(3), 548–557 (June 1999).
21. D. N. Nenchev, K. Yoshida, P. Vichitkulsawat and M. Uchiyama, "Reaction null–space control of flexible structure mounted manipulator systems," IEEE Trans. Robot. Autom. **15**(6), 1011–1023 (Dec. 1999).
22. *Miniature Humanoid Robot [HOAP-2] Manual*, 1st ed., Fujitsu Automation Co., Ltd, Dec. 2004 (in Japanese).
23. Z. Vafa, The Kinematics, Dynamics and Control of Space Manipulators: The Virtual Manipulator concept *Ph.D. Thesis* (Dept. of Mech. Eng. MIT, 1987).
24. M. A. Torres and S. Dubowsky, "Path-planning in elastically constrained space manipulator systems," in *Proceedings IEEE International Conference Robotics and Automation*, Atlanta, GA, (1993) pp. 812–817.
25. D. N. Nenchev, Y. Umetani and K. Yoshida, "Analysis of a redundant free-flying spacecraft/manipulator system," IEEE Trans. Robot. Autom. **8**(1), 1–6 (Feb. 1992).